A Shoelace Antenna for the Application of Collision Avoidance for the Blind Person

Gaosheng Li, Zhihao Tian, Gui Gao, Liang Zhang, Meng Fu, and Yuwei Chen

***Abstract*—A shoelace antenna for the application of collision avoidance for the blind person is proposed for the first time. A thin flexible metal wire is used to fabricate the antenna, which can run along with the shoelace without destroying the shoe or adding extra big structures. According to the investigations, to put the feeding probe at the bottom of the cross point is better than the locations around the string bowknot. To make the shoelace tighter or looser will influence the performance with an affordable variation. The effect of the biological tissues has been taken into account during the performance evaluation of the antenna. The measured fractional bandwidth is 11% with a resonance of 2.43 GHz in the ISM Band. The main lobe of the antenna points to the upper front direction with an angle of about 20 degrees, which is suitable for the detecting of the anterior obstacles when walking. The measured results indicate reasonable performance for the shoelace antenna to serve as a tool for the blind person.**

***Index Terms*—Blind person guidance, collision avoidance, shoelace antenna, wearable antenna.**

I. Introduction

The smart wearable systems are drawing more and more attentions during the recent years. Various portable or embedded electronic devices are being developed to enable the people to be an informatic and automatic platform.

From the websites of some sports clothes suppliers, such as Nike™, Adidas™ and Li Ning™, we can find various smart wearable clothes. The Nike™ hyperdunk series shoes and hyperadapt series clothes are under development. The function of automatically tying and wireless communications will be added. Sport detecting chips and embedded data analyzing together with wireless transmissions are considered by Li Ning™ to enable smart sports. Adidas™ is also developing smart ride series products. Google™ map and GPS are used for navigation and positioning, and the sensors of temperature and pressure are mounted, some of the shoes can "talk", some use vibration devices. Wireless communications with mobile phones are under investigation.

Wearable antennas for common purposed have been widely studied. For example, a planar inverted-F antenna made of woven conductive textiles and of patterns embroidered with conductive wires were proposed [1]. A metallic button is proposed as the transition between the textile antenna and the circuit. This antenna operates in the ISM band.

As for wearable and portable antennas, there have been some investigations. The robustness of a wearable inverted-F antenna with respect to body–antenna separation and human tissue dispersion was reported [2]. An octa-band monopole antenna for mobile phones was proposed, which consisted of a folded metal plate with a lumped-element high-pass matching circuit [3].

Visually impaired people faced with much difficulty in walking. It is helpful to develop intelligent systems to guide them. A smart path guidance robot to assist the blind people was developed [4]. The robot is programmed to follow a path and detect obstacles. A system for facial recognition and detection to satisfy the requirements of the blind people was implemented [5]. The information provided to the user will be brought by a text-to-speech tool, and it can be integrated into video door-phone installations or mobile phones. Assistive navigation using multiple sensors for the blind was investigated [6]. The system acquires social media messages to gauge an event and to create alerts. This method integrates wearable sensors to estimate user location based on metric and landmark localization. Thus, it supports the blind by real-time localization so that the user can travel independently.

A huge shoelace shape antenna was designed as a tool to deal with the frequently coherent fluctuations across the plasma boundary [7]. The antenna is a ladder structure, constructed of lanthanum-doped molybdenum wire rungs wound around alumina tension wheels. The outputs of two amplifiers are combined to drive the antenna. This is the only published paper named shoelace (or shoestring, latchet, etc.) antenna till now. But it is totally different with the proposed design in this paper, no matter for the operation principle or for the constitution of the antenna.

In general, the diversity of the antenna structure together with the radiation pattern is limited, while the performance of them including the gain and the efficiency are not so high as expected. And there are not many kinds of navigation measures for the blind person, especially by the means of radio waves. For further improvement of the assistance for the blind people guidance, we propose an antenna mounted in the shoe with some flexibility of design, aiming for the collision avoidance with a new potential portable tool when walking. A smart radar based on the on-chip sensing modules focusing on the collision avoidance for the blind man could be developed with the help of this antenna.

II. CONFIGURATION AND STRUCTURE

When a blind person walks around, the task of the collision avoidance system is to detect the obstacles ahead, which would probably lie within a distance of 1 m and with the height of more than 20 cm. Thus, an antenna on the shoe with the main

Manuscript received Nov. 16, 2016; revised Apr. 23, 2017; accepted Jun. 17, 2017. Date of publication ** **, 2017. Date of current version ** **, 2017. This work was supported in part by the Natural Science Foundation of China under Grant 61372029.

Gaosheng Li, Gui Gao, Meng Fu and Yuwei Chen are with the College of Electronic Science and Engineering, National University of Defense Technology, Changsha, 410073 China . Gaosheng Li is with the University of Liverpool as a visiting scholar in 2016-2017.

Zhihao Tian is with the Department of Electrical Engineering and Electronics, University of Liverpool, Liverpool, L69 3GJ United Kingdom.

Liang Zhang is with the Department of Biomedical Engineering, the Fourth Military Medical University, Xi'an, 710032 China.

(Corresponding author: (Gaosheng Li e-mail: Gaosheng7070@vip.163.com)

Color versions of one or more of the figures in this communication are available online at http://ieeexplore.ieee.org.

Digital Object Identifier 10.1109/TAP.2017.*******

radiation direction pointing to the upper front and without high side lobes nor a big back lobe is required for the shoe-borne system, as shown in Fig. 1. The transmission of the radar detecting signals together with the catching of the reflection echoes from the obstacles could be implemented by the shoelace antenna. Information of the distance as well as the azimuth angles of the obstacle would be extracted after the signal processing. To produce the equipment with ease, it is helpful to have the operation frequency of the antenna fall into the band of ISM, namely, 2.400 GHz-2.483 GHz.

Fig. 1. Sketch of the application scenario of the shoelace antenna for the collision avoidance.

The antenna is made of a metal wire with a radius of 0.3 mm that runs along with the shoelace, as shown in Fig. 2 (a).

(a)

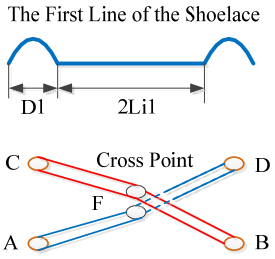

(b)

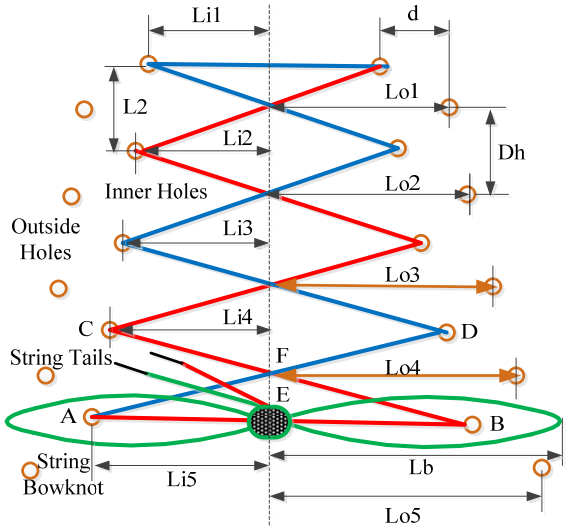

(c)

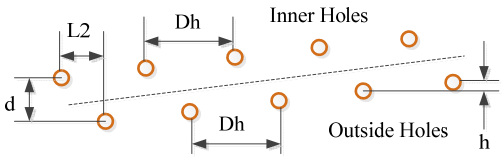

(d)

Fig. 2. Structure of the shoelace antenna. (a) A metal wire mounted along with the shoelace, (b) The first line of the shoelace and the diagram of the cross point, (c) Structure of the central shoelace, and (d) Side view of the two lines of holes for the shoelace.

Where, D1=15 mm, L2=22 mm, Li1=16 mm, Li2=19, Li3=22 mm, Li4=25 mm, Li5=28 mm, Dh=22 mm, Lo1=25 mm, Lo2=28, Lo3=31 mm, Lo4=34 mm, Lo5=37 mm, h=3, and d=9.

Actually, it could be realized by metalizing the shoelace or bury a metal wire in it. There are two semi-circles in the first line of the shoelace and the cross point is not electrically connected, as shown in Fig. 2 (b). Here, the model shoe belongs to Nike™ air Huarache Run 819685, with an outline length of 31.5 cm.

Fig. 2 (c) shows the main structure, indicating totally four crossing points and a string bowknot at the back. There are two lines of holes at each side of the shoe for the fabricating of the shoelace, as shown in Fig. 2 (d). It is worth mentioning that, as shown in Fig. 2 (b), there is a gap between the two lines, and the metal wire is covered by a non-conductive coat. Adding a nonmetal layer will benefit the performance of the antenna according to the simulation results.

A computation model with both the shoe and the human body is built, as shown in Fig. 3. The model of human is generated and exported from the software of Makehuman™, with a total height of 175 cm.

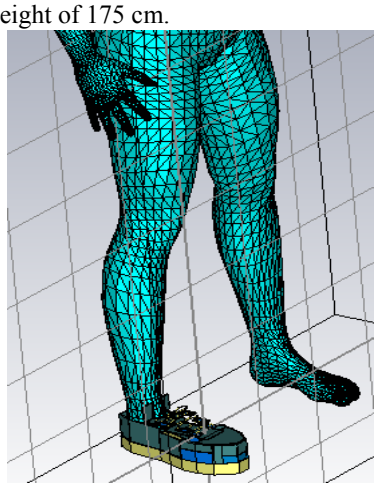

Fig. 3. The model of the shoelace antenna on the shoe together with that of the human body.

III. SIMULATIONS AND ANALYSIS

The feeding point can be located under the center of the string bowknot, as shown in Fig. 4 (a), or at the back of the bowknot, or under the fourth (counted from the tip of the shoe) cross point, as shown in Fig. 4 (b).

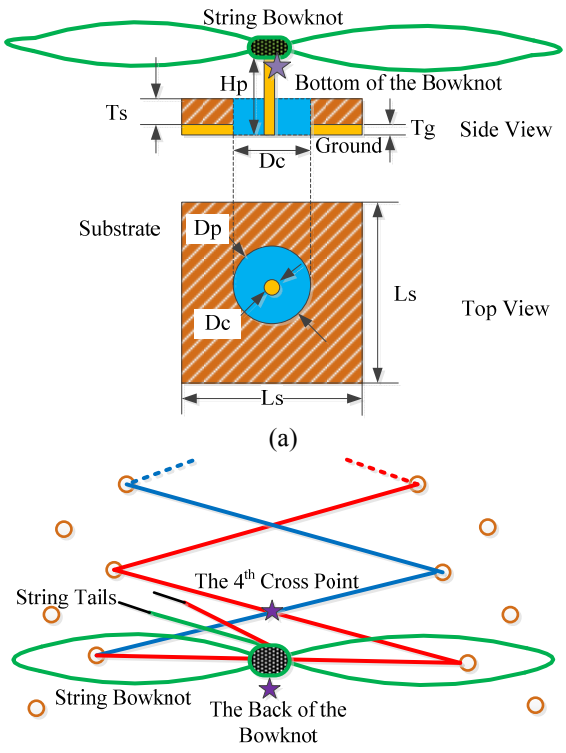

Fig. 4. The string bowknot of the shoe and the feeding structure.

Where, Ls=20 mm, Dc=1.2 mm, Dp=4 mm, Hp=5 mm, Tg=0.035 mm, Ts=2.2 mm.

To get a proper resonance frequency, we simulated a series of parameters of the feeding structure. Many parameters and factors have been considered, including the dielectric permittivity and the size (thickness, length, and width) of the microstrip substrate, the length and the diameter of the probe, etc. They do have some influence on the S11 of the antenna, while the impact on the radiation is not so sharp.

The optimized size of the substrate (Rogers RT5880, with a permittivity of 2.2) is only a little bigger than that of the SMA connector, thus, the space occupation could be reduced for the user. The reflection coefficients at the three different locations are studied with the help of CST MWS.

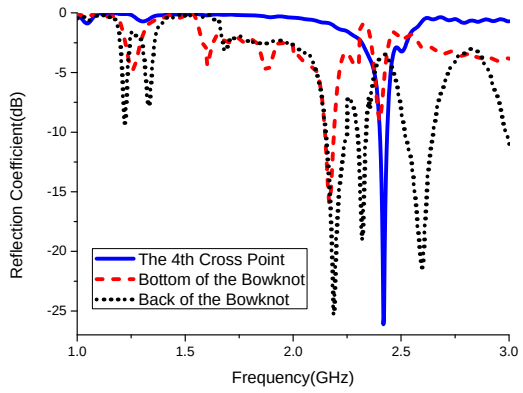

Fig. 5. The simulated reflection coefficients corresponding to three feeding locations.

Fig. 5 shows the calculation results when the feeding point is at the bottom of the string bowknot, at the back of the bowknot or at the bottom of the fourth cross point. As the variation of the feeding point, the reflection structure together with the injection angle would change as well, which bring the different matching performance of the antenna.

This antenna operates like a transformed Yagi-Uda antenna when excited at the cross point. Where, the string bowknot serves as a reflector and the first three cross lines act as the directors. Though the directors are not parallel one by one, they have a macro front pointing direction and could guide the electromagnetic waves towards the tip of the shoe. By the way, the shoelace could be arranged to be other styles within the holes of the shoe, which would provide different radiation characteristics. That would also work, as the simulations carried out by us have proved. The reflectors consist of two thin loops and could push signals to the front efficiently.

TABLE I indicates the influence of some typical parameters (including that of the shoe, the probe and the substrate) for the reflection coefficients and the radiation patterns of the antenna, which is based on a series of simulations for parameter studying, scanning and optimizing.

TABLE I
THE INFLUENCE OF TYPICAL PARAMETERS ON THE ANTENNA PERFORMANCE

Parameters	Reflection coefficient	Radiation pattern
Length of the bowknot	Very small changes observed (less than 5%)	Gets sharper when it grows larger (up to 5% of the 3 dB beam width)
Length of the feeding probe	Would have impact on the S11 and the operating frequency (up to 15%)	Almost no influence (with changes in the amplitude of no more than 1%)
Radius of the shoelace	Not sensitive (changes of no more than 3%)	Not sensitive (un shifted main lobe and side lobes with fluctuations of less than 1% in level)
Horizontal distance of the holes	Slight changes would occur (up to 5%)	Gets narrower in the main lobe when it increases (nearly linear changes for the 3 dB beam width)
Vertical distance of the holes	Slight changes would occur (up to 5%)	Gets narrower in the main lobe when it increases (nearly linear changes for the 3 dB beam width)
Number of the directors	The centric frequency gets small shifts with it (not more than 2%)	The gain would increase with it (by up to 50% for numbers lower than 10)
Permittivity of the substrate	Would push the resonance frequency from low to high (quasi-linear increasing)	Tiny impact (changes of no more than 2% for the gain values)

In the above design, a resonance frequency of 2.43 GHz can be obtained here, with a bandwidth of 40 MHz (2.41 GHz-2.45 GHz). It would be 2.2 GHz when the location is changed to the bottom of the bowknot, while that at the back of it would bring several operation bands below 3 GHz. The structure of the shoe is built in the calculations using materials of rubber of cloth, and the ground is substituted by a metal cuboid with the dimensions of 400 mm×300 mm×4 mm. The whole body of the human is taken into the scope of the computation as the

radiation background to embody the influence of the operating environment.

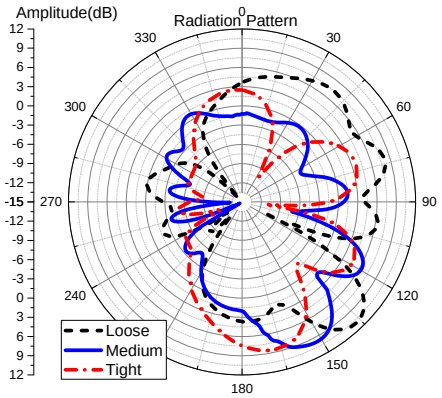

Fig. 6. Radiation patterns of the three status of the shoelace (H-plane).

According to the structure of the shoe, we define three statuses of the shoelace, namely, loose, medium and tight, which represents to fabricate the shoelace and the metal wire into the outer holes, into the inner holes and to make further fastening at the inner holes. The excitation is fed at the 4th cross point. The radiation patterns corresponding to the three statuses in the H-plane are shown in Fig. 6. Here, the plane is the one of vertical polarization, which is perpendicular to the ground.

The main radiation angle of the three configurations (loose, medium and tight) is 58° , 25° and 4° from the front ground surface, respectively (corresponding to 122°, 155° and 176° in the figure). The angle decreases while the gain increase slightly.

TABLE II
THE MAIN LOBE WIDTH AND THE GAIN OF DIFFERENT STATUS OF THE SHOELACE (H-plane)

Status of the shoelace	Main lobe (°)	Gain (dBi)
Tight	176	8.57
Medium	155	9.73
Loose	122	10.94

As shown in TABLE II, the gain of the medium status is 9.73 dBi and this would be the mainly used configuration, since there is a large main lobe in the front while only two small side lobes pointing to the empty that would probably not bring false alarms.

The horizontal radiation patterns of the antenna are shown in Fig. 7, which is in parallel with the ground. The gains are fairly low due to the feature of upper directivity of the antenna.

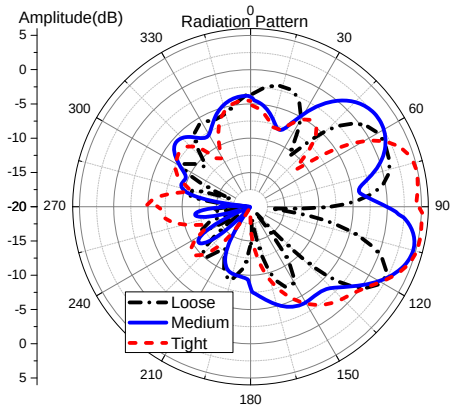

Fig. 7. Radiation patterns of the three status of the shoelace (E-plane).

A different insight into the radiation could be achieved from the cut slice of the main radiation angle of the three statuses, as shown in Fig. 8.

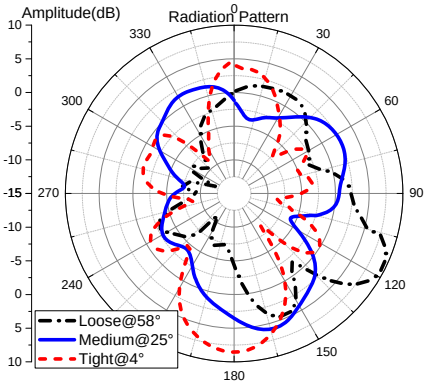

Fig. 8. Radiation patterns of the three status of the shoelace (the slice of the main radiation direction at each status, namely 58°, 25° and 4°, respectively).

The 3 dB beam width and the gain corresponding to the statements of loose, medium and tight are shown in TABLE III.

TABLE III
THE 3 dB BEAMWIDTH AND THE GAIN ACCORDING TO DIFFERENT STATUS OF THE SHOELACE AT THE SLICE OF THE MAIN RADIATION DIRECTION

Status of the Shoelace	3 dB Beam width (°)	Gain (dBi)
Tight	36.1	9.50
Medium	39.0	6.52
Loose	25.5	9.07

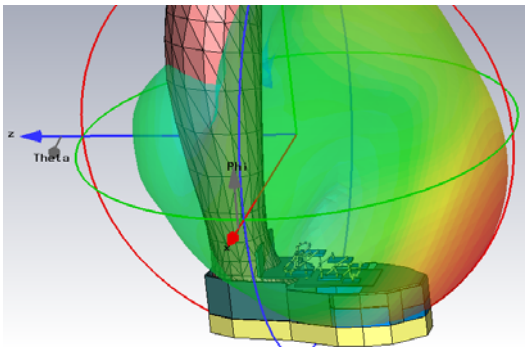

Fig. 9. The 3 D radiation pattern of the shoelace antenna at 2.43 GHz when excited at the fourth cross point.

Fig. 9 is the 3 D radiation pattern of the shoelace antenna at the medium status of the shoe string, from which the upper front feature of the radiation directivity can be observed. Both the shoe and the leg together with the colorful field distribution could be seen. Here, the E-plane is parallel to the ground. That is, the bottom of the shoe. And the H-plane is vertical to the ground.

To make it more clearly about the influence of the biological tissues on the antenna performance, a comparison of the reflection coefficients when with or without the human body is shown in Fig. 10. Only slight differences could be seen from the two curves, no matter for the resonance frequency or the absolute values of the return losses among 1.0 GHz-3.0 GHz.

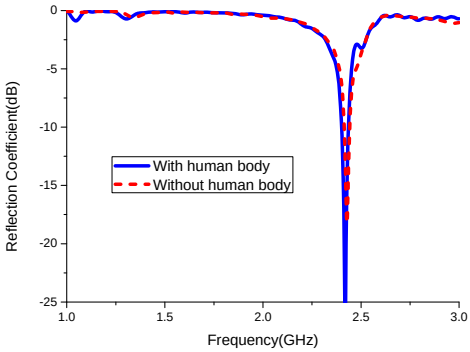

Fig. 10. Comparison of the reflection coefficients considering the effect of the biological tissues.

Furthermore, the comparison of the radiation patterns is presented in Fig. 11. The two patterns are similar in shape whether there is a model of human body or not. A deviation of 3° for the main radiation azimuth could be observed between the two scenarios.

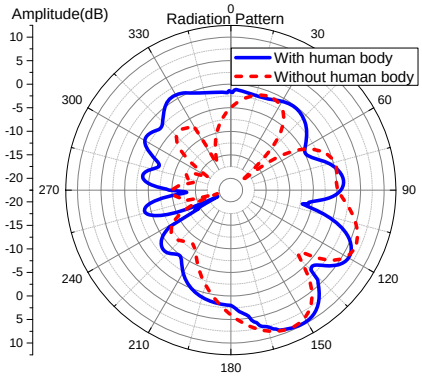

Fig. 11. Comparison of the radiation patterns considering the effect of the biological tissues.

IV. MEASUREMENT AND RESULTS

A shoelace antenna is fabricated and measured for verification. The materials and the parameters of the substrate and the radiation body is selected according to the former description. The feeding location is at the bottom of the fourth cross point. For the measurement of the reflection coefficients and the radiation patterns, a vector network analyzer (VNA), Anritsu 37369A, is used to get the curves.

To imitate the real application scenario better, a prosthesis of a foot and a piece of leg for medical training is put into the shoe. The following measurements are based on the statement of medium length of the shoelace.

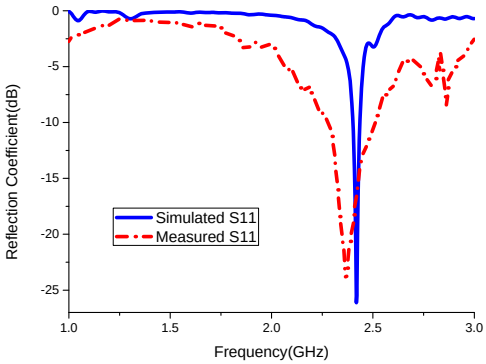

Fig. 12. Comparison of the simulated and the measured results of S11 curves at 2.43 GHz.

Fig. 12 presents the comparison of the simulated and the measured S11 curves from 40 MHz to 3.0 GHz. The measured center frequency is 2.34 GHz, and the operation range is 2.22 GHz-2.48 GHz, which covers that of the simulated results. According to the simulated 2.43 GHz, there are some differences occurred, which are mainly brought by the gap between the simulation setup and the measurement scenario, including the simplification of the geometry of the shoe and the human body, as well as the non-ideal measurement configuration.

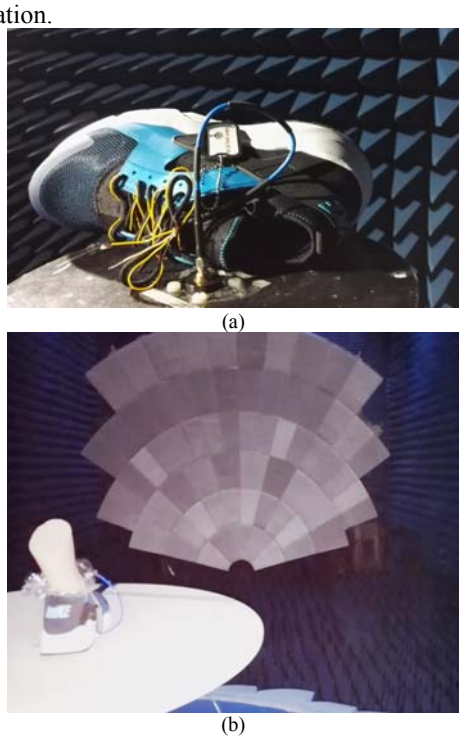

(a) (b)

Fig. 13. Measurement of the radiation patterns of the shoelace antenna in the anechoic chamber. (a) Photography of the shoelace antenna on the turntable, (b) The shoelace antenna with a prosthesis of foot and a piece of leg in the compact range chamber.

The radiation patterns are measured in the anechoic chamber with the help of a turntable and the VNA, as shown in Fig. 13 (a). The whole structure is measured in a compact range chamber with a paraboloid reflector, as shown in Fig. 13 (b).

Fig. 14 presents the comparison of the simulated and the measured radiation patterns of the shoelace antenna at 2.43 GHz in vertical polarization. The measured shape of the radiation pattern is similar to that simulated, especially for the direction of the main lobe, though there are some differences in the values of the rises and falls, which would probably be introduced by the antenna shape deformation due to the manual fabrication. Moreover, the prosthesis used in the measurement is only a foot and a piece of a leg. It is not the same as the simulation configuration, which would also bring some impact for the gaps between the two curves.

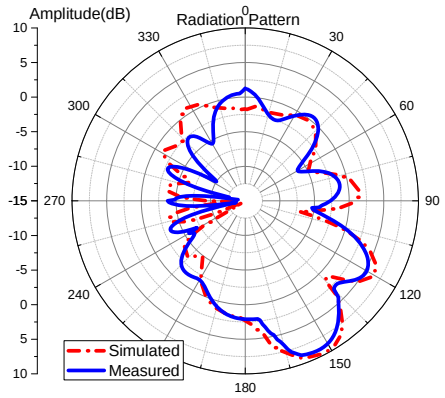

Fig. 14. Comparison of the simulated and the measured radiation patterns of the shoelace antenna.

V. Conclusion

The simulations and measurements demonstrated the validation of the shoelace antenna. The certain operation requirement of the guidance for the blind people could be satisfied owe to the fairly large size and a proper excitation. Thus it offers a proper tool for the development of the collision avoidance radar. Furthermore, the shoelace antenna could serve as a general purpose front end and is a promising candidate for the applications of WLAN, navigation and positioning, body-centric networks, sports and healthcare monitoring, etc.

References

[1] Branimir Ivsic, Davor Bonefacic, and Juraj Bartolic, "Considerations on Embroidered Textile Antennas for Wearable Applications," *IEEE Antennas and Wireless Propa. Letters*, vol. *12,* pp. *1708-1711*, 2013.

[2] G. A. Casula, A. Michel, P. Nepa, G. Montisci, and G. Mazzarella, "Robustness of Wearable UHF-Band PIFAs to Human-Body Proximity," *IEEE Trans. on Antennas and Propagation*, vol. 64, No. 5, pp. *2050-2055,* 2016.

[3] Yan Wang and Zhengwei Du, "Wideband Monopole Antenna with Less Nonground Portion for Octa-Band WWAN/LTE Mobile Phones," *IEEE Trans. on Antennas and Propagation*, vol. 64, No. 1, pp. 383–388, 2016.

[4] Siti Fauziah Toha, Hazlina Md Yusof, Mohd Fakhruddin Razali and Abdul Hadi Abdul Halim, "Intelligent Path Guidance Robot for Blind Person Assistance," in *Proc. 4th ICIEV,* Kitakyūshū, Japan, 2015, pp. 100–104.

[5] A. Fernández, J. L. Carús, R. Usamentiaga and R. Casado, "Face Recognition and Spoofing Detection System Adapted To Visually-Impaired People," *IEEE Latin America Trans.*, vol. 14, No. 2, pp. 913–921, 2016.

[6] Samleo L. Joseph, Jizhong Xiao, Xiaochen Zhang, Bhupesh Chawda, Kanika Narang, Nitendra Rajput, Sameep Mehta, and L. Venkata Subramaniam, "Being Aware of the World: Toward Using Social Media to Support the Blind With Navigation," *IEEE Trans. on Human-Machine System*, vol. 45, No. 3, pp. 399–405, 2015.

[7] W. Burke, T. Golfinopoulos, B. LaBombard, R.R. Parker, and W. Parkin, P. Woskov, "The Shoelace antenna: A Device for inductively coupling to low frequency, short wavelength fluctuations in the plasma boundary," in *Proc. 26th SOFE,* Austin, USA, 2015, pp. 171–175.